MATERIALS SCIENCE

2016 © The Authors, some rights reserved; exclusive licensee American Association for the Advancement of Science. Distributed under a Creative Commons Attribution NonCommercial License 4.0 (CC BY-NC).
10.1126/sciadv.1501297

Shape memory polymer network with thermally distinct elasticity and plasticity

Qian Zhao, Weike Zou, Yingwu Luo, Tao Xie*

Stimuli-responsive materials with sophisticated yet controllable shape-changing behaviors are highly desirable for real-world device applications. Among various shape-changing materials, the elastic nature of shape memory polymers allows fixation of temporary shapes that can recover on demand, whereas polymers with exchangeable bonds can undergo permanent shape change via plasticity. We integrate the elasticity and plasticity into a single polymer network. Rational molecular design allows these two opposite behaviors to be realized at different temperature ranges without any overlap. By exploring the cumulative nature of the plasticity, we demonstrate easy manipulation of highly complex shapes that is otherwise extremely challenging. The dynamic shape-changing behavior paves a new way for fabricating geometrically complex multifunctional devices.

Shape shifting in response to environmental changes is commonplace in nature. Its diversity and the associated functions are crucial for nature's survival (*1*). Stimuli-responsive shape-shifting polymers with similar intelligence have attracted tremendous attention owing to their vast technological potential (*1*). In particular, the drive for discovering ever more diverse shape-shifting behaviors that match or even exceed the complexity of natural systems appears to be a never-ending task (*2*–*7*). Shape memory polymer (SMP) is a unique class of such polymers for which externally programmed shape(s) can be temporarily fixed and later recovered on demand (*8*–*10*). Realization of its vast practical potential in a number of technological areas including deployable structures (for example, biomedical and aerospace) (*11*) and functionally tunable devices (*12*, *13*) has stimulated intense interests in this area. Recent discovery of triple-shape (*14*), multiple-shape (*15*, *16*), and reversible shape memory (*17*) beyond the classical dual-shape behavior has reshaped the landscape in this field, yet all shape memory behaviors share a common root in polymer elasticity, with the basis being the storage and release of entropic energy via chain conformation changes (*8*–*10*). An opposite behavior—polymer plasticity, which refers to reshaping polymers permanently without macroscopic melting—has recently gained attention (*18*–*26*). Mechanistically, this is achieved by covalent bond exchange in a polymer network, allowing its topography to be rearranged in response to an external force. That is, the shape change is not accompanied by chain conformation (or entropy) change and is thus permanent (that is, nonrecoverable). This particular property is fundamentally different from the commonly known reprocessing of thermoplastic polymers in its fluidic state (that is, plastic flow) in that the permanent reshaping can occur while the material maintains its dynamic crosslinking state. This difference has been proven quite beneficial because it leads to a new range of exciting possibilities including malleability of thermoset polymers (*21*–*25*), mechanopatterning of elastomers (*19*), and mechanical orientation of liquid crystalline elastomers (*26*).

Whereas elasticity-based shape memory behaviors allow erasing prior shapes for many cycles of shape (re)programming (that is, noncumulative), polymer plasticity is cumulative (*19*, *20*), referring to the fact that permanently reshaping polymers via plasticity can be repeatedly done without losing the previous strain history, opposite to the elasticity-based shape memory effect. Plasticity may be triggered thermally (*20*–*26*) or by light exposure (*18*, *19*, *27*). Although light-induced plasticity has its own merits (for example, spatio-selectivity), it has intrinsic drawbacks, notably the need for line-of-sight access and limited light penetration depth, both of which prohibit its use for three-dimensional (3D) bulk systems. In addition, the reliance on consumable initiators to trigger light-induced plasticity does not allow many cycles of shape manipulation. In the absence of the cumulative effect of plasticity, an SMP network with plasticity, despite its mechanistic uniqueness, from practical shape manipulation standpoint is not different from a thermoplastic SMP because the permanent shape of the latter can also be redefined but the prior shape(s) would be completely erased.

The limitations of light-induced plasticity are largely inapplicable for thermally triggered systems. With this and other considerations in mind, we set out to design an SMP network with thermally distinct elasticity and plasticity, with particular attention to achieving a cumulative effect for the latter as the key for complex shape manipulation. Such a network should have a shape memory transition. In addition, it should have its plasticity induced at a temperature [plasticity temperature (T_p)] sufficiently above the shape memory transition temperature (T_{trans}) to completely separate the elasticity and plasticity. The design principle of the target system is illustrated in Fig. 1A. The network contains molecular chain segments that can be chosen to tailor the T_{trans} and reversible (exchangeable) covalent bonds that can be activated at a corresponding T_p. The left-hand route in Fig. 1A shows its elasticity-based shape memory behavior. At a relatively low temperature of T_1 ($T_{trans} < T_1 < T_p$), the molecular chain mobility is activated but the reversible covalent bonds remain dormant. At this state, any deformation upon application of an external stress should lead to chain conformation change, cooling under the load results in fixation of the deformed shape, which can be recovered upon reheating because of the entropic nature of the shape change. The same network, when deformed at T_p, is expected to show plasticity. As shown in the right-hand route in Fig. 1A, reversible covalent bonds become activated at T_p, applying an external force which results in network topographic change via bond exchange. The deformed shape is not associated with any entropic change; thus, the shape change is nonrecoverable or permanent.

A crucial factor to consider is that typical plasticity systems are induced at temperatures that are either too low to accommodate a shape

State Key Laboratory of Chemical Engineering, College of Chemical and Biological Engineering, Zhejiang University, Hangzhou 310027, China.
*Corresponding author. E-mail: taoxie@zju.edu.cn

Downloaded from http://advances.sciencemag.org/ on January 26, 2016

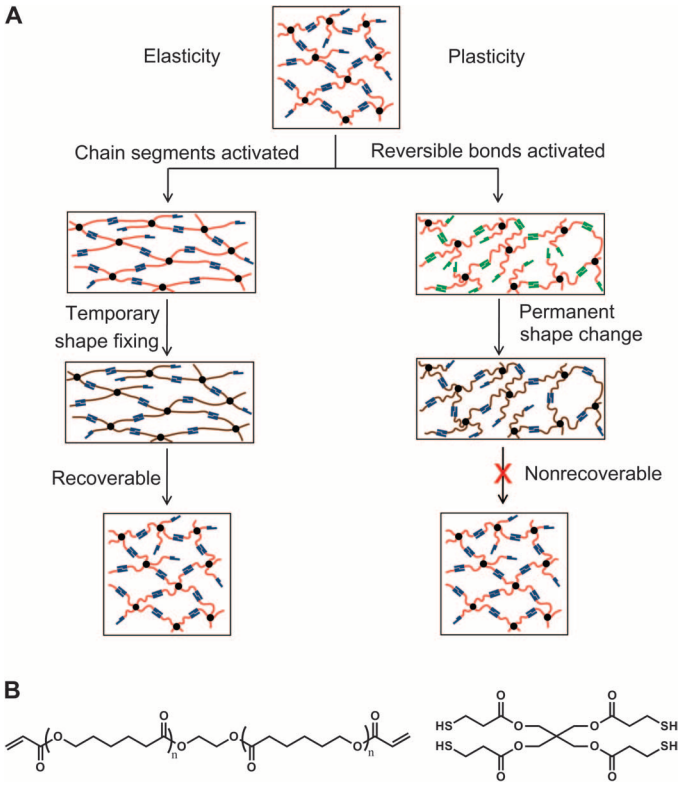

Fig. 1. Design of network with thermally distinct elasticity and plasticity. (**A**) Schematics of the physical molecular principle. Black dots represent permanent crosslinking points; green and blue colors represent the activated and nonactivated states of the reversible bonds, respectively; and red and dark gray lines represent the activated and nonactivated states of the chain segments, respectively. (**B**) Precursor monomers for the network synthesis.

memory transition or too high to not endanger the network via thermal degradation upon repeated and prolonged heating at T_p. By contrast, T_{trans} for an SMP can typically be tuned in a wide temperature range owing to many years of development in the field; thus, the need to have an appropriate T_p is more the focus of the current study.

A crosslinked poly(caprolactone) (PCL) system was chosen as the model network to realize the thermally distinct elasticity and plasticity outlined in Fig. 1A. The network was synthesized by a radical initiated reaction between PCL-diacrylate (PCLDA) and a tetrathiol crosslinker (Fig. 1B). We emphasize that this is an SMP chemistry previously documented by Rodriguez *et al.* (*28*). The particular focus of the current study is to induce thermal plasticity in such a network with a transesterification catalyst. For such a system, the melting transition of PCL (55°C) serves as the basis for the shape memory elasticity, whereas the transesterification reaction catalyzed by a neutralized organic base [1,5,7-triazabicyclo[4.4.0]dec-5-ene (TBD)] is expected to contribute to its plasticity. Because of its strong basicity for catalyzing thiol-ene Michael addition reaction, TBD needed to be neutralized to prevent instantaneous gelation during the network synthesis. As revealed later in the context, the neutralized TBD was quite effective to induce plasticity. Here, the choice of PCL was also critical because the high density of the ester linkages in the network may promote the bond exchange kinetics to lower T_p from typical transesterification systems (*21*, *23*), a beneficial factor to achieve a robust cumulative plasticity effect. We recall here that PCL has been widely used in designing SMP (*28*, *29*), yet triggering the transesterification reaction with a catalyst to induce plasticity in an SMP network has not been attempted before.

The thermally induced plasticity of the network was first investigated via iso-strain stress relaxation. In this set of experiments, each sample was stretched to 100% strain. We emphasize that this strain value is much higher than those reported for other transesterification-based plasticity systems (~10%) (*21*, *23*, *25*). This is particularly important given our interest in shape changing instead of malleability in those studies. Nevertheless, with the strain maintained constant, the stress relaxation (σ/σ_0) was monitored, with σ and σ_0 representing the instantaneous stress and the initial stress, respectively. Figure 2A shows that complete stress relaxation at 150°, 140°, 130°, 120°, and 110°C takes about 10, 20, and 40, 100, and 200 min, respectively. Thus, 130°C is an appropriate temperature of choice to achieve plasticity because it allows complete stress relaxation within a reasonable time without concerns about the thermal degradation of typical polymers. This temperature is sufficiently above the T_{trans} of typical SMPs (*8*–*10*), including that of the current system. We therefore use this temperature to further probe the thermally distinct elasticity and plasticity. We should state here that T_p is not a static temperature; the transesterification reaction does occur at temperatures below 110°C. However, the reaction may become so slow that it can be neglected. Thus, T_p is defined as the experimental temperature at which the plasticity is induced at a rate that is significant within the experimental time scale.

We note here that similar iso-strain stress relaxation experiments were typically used to quantify plasticity and malleability in the literature (*21*, *23*). Our purpose of introducing plasticity is quite different in that we are more interested in permanently changing the shape of a polymer instead of reprocessing thermosets. Thus, a parameter that is more relevant than stress relaxation has to be identified. Such a parameter is defined as the shape retention ratio $R_{ret} = 100\% \times \varepsilon/\varepsilon_{load}$, with ε_{load} and ε representing the respective strains at the plasticity temperature before and after load removal, respectively. We note that the shape fixity ratio for a typical elastic shape memory cycle is defined by a seemingly similar equation $R_f = 100\% \times \varepsilon/\varepsilon_{load}$. The critical difference lies in that ε in R_f refers to the temporarily fixed strain (recoverable), whereas ε in R_{ret} is the permanent strain (irrecoverable).

A question naturally arises: How is the stress relaxation quantitatively related to R_{ret}? To answer this question, a sample was subjected to partial stress relaxation experiments summarized in Fig. 2B. In this type of experiments, the sample was first stretched to 100%. While maintaining this strain value, partial stress relaxation was allowed by controlling the relaxation time. The external stress was then removed, and the sample was allowed to reach its equilibrium length. This completes the first stress relaxation experiment, and the equilibrium length is used to calculate the R_{ret} corresponding to this particular extent of stress relaxation [$R_\sigma = 100\% \times (1 - \sigma/\sigma_0)$]. Subsequently, three more stress relaxation cycles were run on the same sample in a similar fashion: stretching it to 100% strain and allowing the stress to relax to a higher extent in each cycle. The correlation between R_{ret} and R_σ can thus be obtained. Figure 2C shows that R_{ret} typically falls behind R_σ, but the lag between the two becomes smaller and smaller as the stress relaxation approaches 100%. An R_σ value of 90%, for instance, corresponds to an R_{ret} value of mere 80%, and full shape retention ($R_{ret} \approx 100\%$) can only be achieved when the stress is completely relaxed ($R_\sigma \approx 100\%$).

As mentioned earlier, achieving a robust cumulative plasticity effect requires that the network can undergo multiple cycles of stress relaxation

Downloaded from http://advances.sciencemag.org/ on January 26, 2016

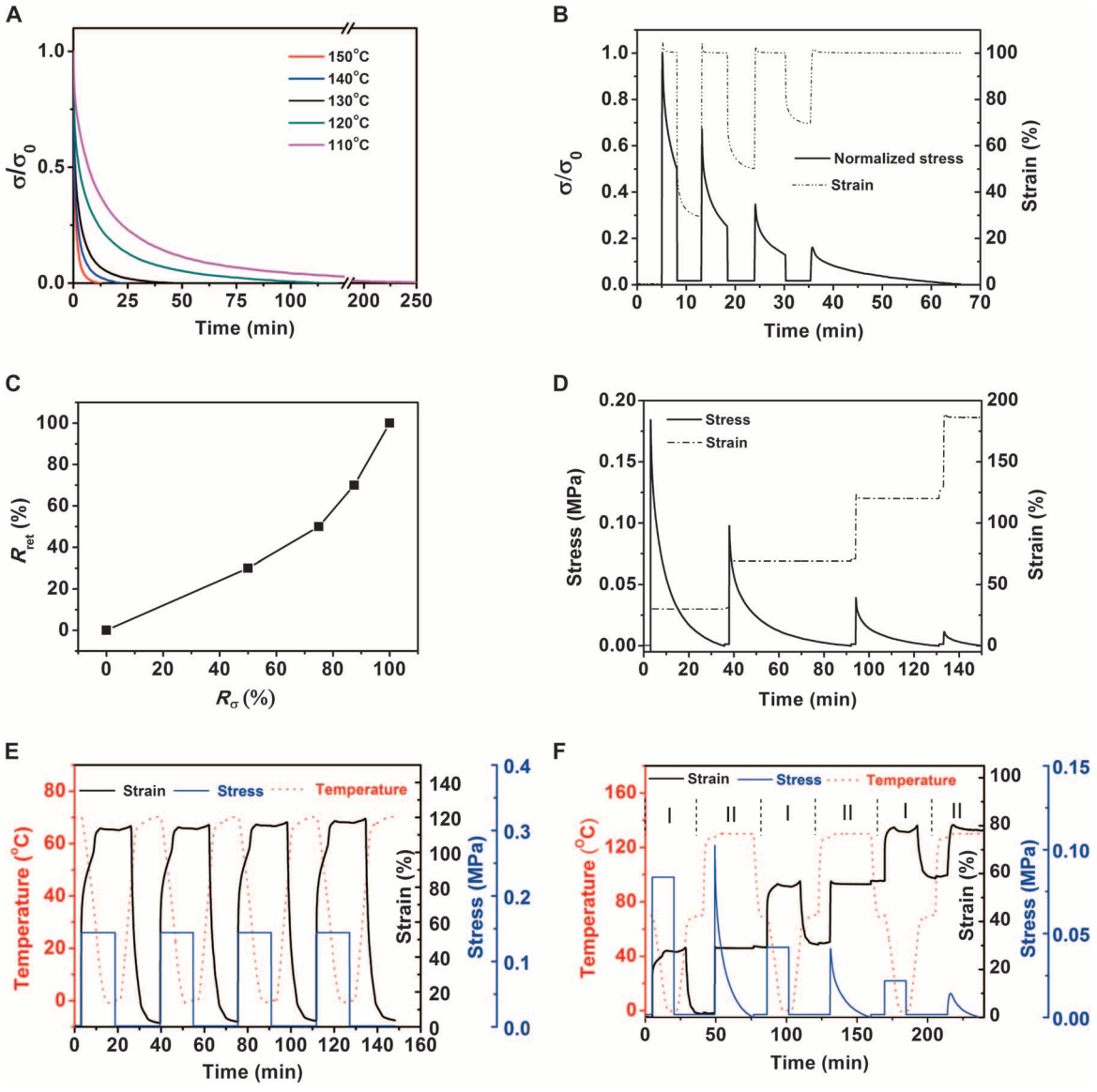

Fig. 2. Thermomechanical characterization of the elasticity and plasticity. (**A**) Stress relaxation at various temperatures. (**B**) Partial stress relaxation and the corresponding shape retention at 130°C. (**C**) Quantitative correlation between the shape retention ratio and the extent of stress relaxation. (**D**) Consecutive plasticity (stress relaxation) cycles at 130°C. (**E**) Consecutive elasticity (shape memory) cycles. (**F**) Consecutive elasticity and plasticity cycles (labeled "I" and "II," respectively, for easy demonstration).

(and shape retention) without deterioration in its performance. This was probed by four consecutive stress relaxation cycling experiments summarized in Fig. 2D, showing that the stresses can be completely relaxed in all cycles. This is nontrivial because an otherwise higher T_p may induce various side reactions that could lead to either material brittleness (strain reduction) or permanent crosslinking that could destroy the plasticity. We note that the peak stress in each cycle in Fig. 2D decreases progressively with the cycling. This is partly due to the fact that the stress values were calculated on the basis of the initial sample cross-section area, whereas the actual cross-section areas for subsequent cycles were progressively lower because of the cumulative sample elongation. Mullin's effect may be another reason for the cycle-to-cycle reduction in peak stress.

Having established the basis for plasticity, we evaluated the elastic shape memory performance of the network. The consecutive shape memory cycles in Fig. 2E were obtained under a stress-controlled mode with identical deformation and recovery temperatures of 80°C. Within each cycle, the shape fixity ratio and shape recovery ratio are both above 98%. Cycle-to-cycle comparison shows very little deviation. The overall strain shift even after four consecutive cycles is quite minimal (about 2%). These results suggest that plasticity is suppressed under the condition of the elastic shape memory experiments.

The above experiments set the basis for probing thermally distinct elasticity and plasticity in one combined thermomechanical cycle. Figure 2F shows four consecutive elasticity/plasticity cycles. Within each cycle, an elasticity-based shape memory cycle was achieved with the

Downloaded from http://advances.sciencemag.org/ on January 26, 2016

shape fixity and shape recovery ratio both above 98%, followed by a plasticity cycle with the shape retention ratio approaching 100%. No noticeable deterioration in performance (shape retention for plasticity and shape fixing and recovery for elasticity) was observed upon cycling. These results verify that the plasticity and elasticity can be realized in a highly robust fashion without any overlap.

The thermally distinct plasticity and elasticity offer unprecedented flexibility in 3D shape manipulations. Figure 3A shows that a square film can be folded plastically into a permanent bird, which can be deformed into various temporary shapes (a plane or a flat film) that can recover by virtue of its elasticity. The recovered bird can be further manipulated plastically to form a drastically different permanent origami structure (boat) that can also fix various recoverable temporary shapes (a windmill or a flat film). This ability to repeatedly and permanently redefine the shape of a smart origami is a critical distinction from other known responsive origami structures (*30*, *31*). Another distinction lies in that typical smart origami requires more complicated fabrication processes that often involve the use of multiple material sets (*30*, *31*), whereas the current system consists of a single material with the most straightforward folding and stress relaxation process. Similarly, with cutting, folding, and plastic deformation, a rectangular flat film can be used to create a kirigami structure that can also be deformed into recoverable temporary shapes (Fig. 3B). Movies showing the shape recovery of various origami and kirigami structures can be found in the Supplementary Materials (movies S1 to S5). Here, the importance of the recovery into complex 3D permanent shapes can be easily overlooked. Conventional shape memory behaviors allow a permanent flat film to be deformed into a temporary 3D shape, and thus the recovery of the latter back into the former (complex to simple). The opposite geometric change (recovery to a complex shape) requires the fabrication of a complex permanent shape, which is beyond the scope of conventional shape memory concepts. The recovery into complex permanent shapes is highly relevant practically because many SMP device applications do involve 3D permanent geometries. To further emphasize the advantage of the thermally induced plasticity, we note that the 3D permanent shapes in Fig. 3 are difficult to fabricate by light-induced plasticity because of its line-of-sight limitation.

The cumulative nature of the plasticity provides an additional unique freedom for shape manipulation. The images on the left-hand side of Fig. 4A demonstrate that a flat film can be plastically deformed five times to yield an arbitrarily defined permanent tube with surface features on its internal wall, which is nearly impossible to fabricate with conventional processing techniques. Such a complex final shape is the direct consequence of the cumulative plasticity; that is, the deformation introduced in each plasticity step was carried over to the final structure. Here, each of the intermediate permanent shapes can also be elastically programmed into recoverable temporary shapes (images on the right-hand side of Fig. 4).

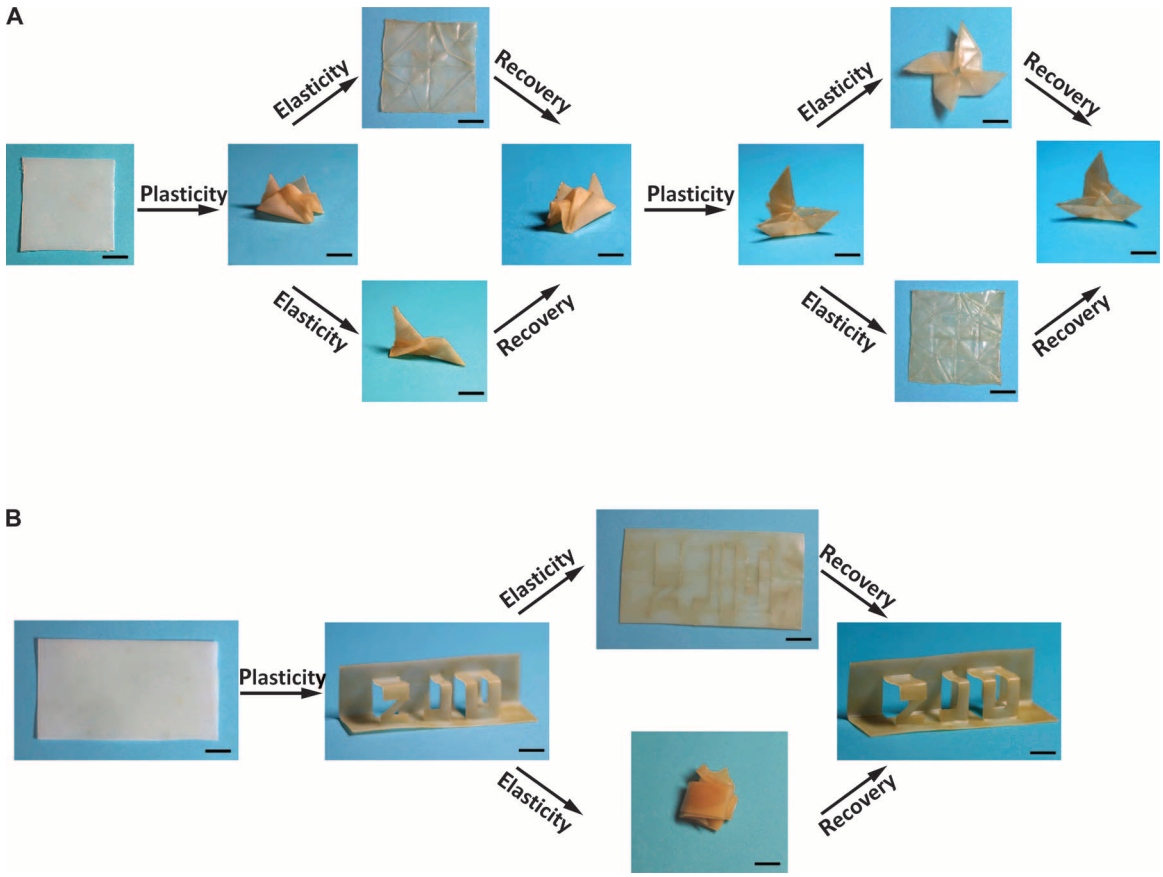

Fig. 3. Shape manipulation via thermally distinct elasticity and plasticity. (**A**) Smart origami structures. (**B**) Smart kirigami structure. Scale bars, 10 mm.

Downloaded from http://advances.sciencemag.org/ on January 26, 2016

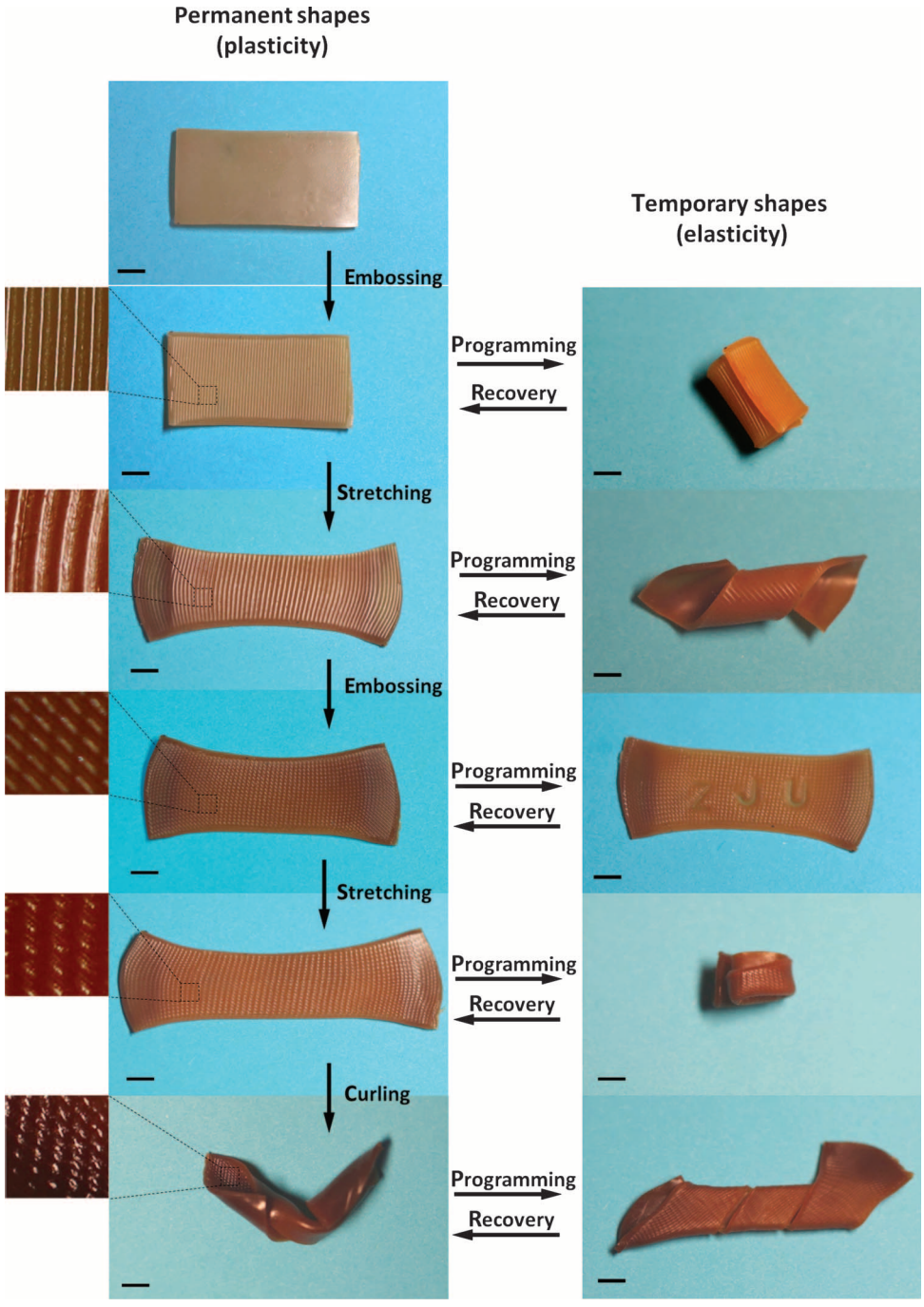

Fig. 4. Demonstration of complex shape manipulation via cumulative plasticity effect and shape memory effect. The original and recovered shapes in each elastic shape memory cycle shown are visually indistinguishable; thus, the same photo was used for ease of demonstration. Scale bars, 5 mm.

We note here that a conventional thermoplastic SMP can be molded and remolded to redefine its permanent shape. However, there are several critical differences between the current system and a thermoplastic SMP. The repeated and complete stress relaxation shown in Fig. 2D, for instance, cannot be achieved with a conventional thermoplastic SMP. A thermoplastic SMP can completely relax its stress only when it is heated to its flow state; however, the material will lose its integrity altogether. Thus, a stable zero-stress state without loss of material integrity, as is accomplished in the repeated stress relaxation in a DMA apparatus (Fig. 2D), is only possible with the dynamically crosslinked system. When a thermoplastic SMP is remolded, the prior shape is completely erased (that is, noncumulative). In contrast, Fig. 4 shows that new permanent deformations are introduced one after another without erasing the prior deformation. Thus, the surface textures from the two embossing steps are

Downloaded from http://advances.sciencemag.org/ on January 26, 2016

preserved in the inner walls of the final arbitrary tube. Had this been a thermoplastic SMP, the surface textures would have been lost as the permanent shape was redefined. Thus, the cumulative effect is a critical factor that distinguishes our system from a thermoplastic SMP. In addition, redefining the permanent shape of a thermoplastic SMP typically requires a mold. Thus, to fabricate the bird and boat in Fig. 3A using a thermoplastic SMP is extremely difficult because this would require a sophisticated mold and demolding would be nearly impossible given the complexity of the shapes involved. We should state that, for thermoplastic SMP, stress can also relax under iso-strain conditions at an elevated temperature below its flow temperature (*32*, *33*). At first glance, this is similar to the essential stress relaxation behavior in Fig. 4D. However, there are fundamental differences: (i) the equilibrium stress cannot reach zero for thermoplastic SMP and (ii) upon heating, the fixed strain after the stress relaxation can recover. The latter is particularly critical because it suggests that such deformation for thermoplastic SMP is elastic instead of plastic, as is observed in our system. Overall, the demonstrations in Figs. 3 and 4 are only possible with our dynamic crosslinked system and are not possible with a thermoplastic SMP. We further note that 3D printing could, in principle, produce polymer devices with largely unlimited permanent geometries into which shape memory functions could also be incorporated. A permanent shape fabricated by 3D printing is, however, static. That is, it cannot be further changed after fabrication. In contrast, the method revealed in this study allows numerous cycles of manipulation of a permanent shape. Despite this fundamental difference, our concept could be combined with 3D printing to yield a 3D permanent shape that could be dynamically manipulated in an on-demand fashion.

In summary, we designed a polymer network with a thermal phase transition and thermally exchangeable covalent bonds. The former introduces elasticity responsible for its shape memory behavior, and the latter contributes to an opposite plasticity via network topography rearrangement. Although both are triggered thermally, they can be reflected distinctively without any overlap. The robustness of the elasticity and plasticity in our system, in combination with the cumulative nature of the latter, permits manipulation of polymer shapes in ways that are limited largely only by imagination. The physical principle behind our system can be readily expanded to a variety of other systems with different phase transitions and reversible covalent chemistry. Thus, our work should lead to numerous opportunities for future innovations involving shaping polymers.

MATERIALS AND METHODS

Materials

Pentaerythritol tetrakis(3-mercaptopropionate) (tetrathiol crosslinker, Sigma-Aldrich), 1-benzoylcyclohexanol (UV-184, photoinitiator, TCI), polycaprolactone diol (M_n = 10,000, Sigma-Aldrich), acryloyl chloride (TCI), and triethylamine (Aladdin) were all used as received. TBD (transesterification catalyst, TCI) was neutralized with 2 molar equivalents of acetic acid before its use. Polycaprolactone diacrylate (PCLDA) was synthesized according to the method reported in the literature (*34*).

Polymer network synthesis

PCLDA (1.5 g) was dissolved in DMF (*N*,*N*′-dimethylformamide) (0.5 g) at 80°C. A DMF solution containing a stoichemical amount of the tetrathiol crosslinker, photoinitiator (UV-184, 0.5 wt %), and neutralized TBD (2 wt %) was added to the PCLDA solution and stirred for several minutes. The precursor solution was quickly poured into a mold defined by two glass slides separated by a silicone rubber spacer (thickness: 0.5 mm). The mixture was then irradiated under ultraviolet light for 5 min (light source: IntelliRay 600 Flood UV, intensity: 30 mW/cm^2). The obtained film was vacuum-dried (100°C) overnight. General material characterizations are available in the Supplementary Materials (fig. S1 to S3).

Thermomechanical characterization

Samples were cut into rectangular shapes (6 mm × 1.5 mm × 0.47 mm) before testing. Unless otherwise noted, tests were conducted with a Dynamic Mechanical Analysis machine (DMA800) in a strain rate mode.

Demonstration of macroscopic shape manipulation

The various origami and kirigami structures were manually folded (or cut for the latter) from flat films. The folded objects were placed between two glass slides and thermally annealed under compression (130°C, ~30 min). Before annealing, silicon oil was spread onto the film surfaces to avoid self-sticking. For the demonstration of the cumulative plasticity in Fig. 4, a flat film was first compressed using a stainless steel mold with a rectangular wave pattern. Then, the film was stretched 30% followed by compression using the same mold rotated by 45°. After a further 30% stretching, the film was curled and bent into a random tube with the surface pattern on its inner surface. Each step above required a thermal annealing (130°C, 60 min) to induce the plasticity. The demonstration of the elastic shape memory behaviors in Figs. 3 and 4 was conducted with an identical deformation and recovery temperature of 80°C following typical shape memory procedures.

SUPPLEMENTARY MATERIALS

Supplementary material for this article is available at http://advances.sciencemag.org/cgi/content/full/2/1/e1501297/DC1

Movie S1. Recovery from an origami boat into an origami bird with infrared heating.
Movie S2. Recovery from an origami plane into an origami bird with infrared heating.
Movie S3. Recovery from an origami windmill into an origami boat with infrared heating.
Movie S4. Recovery from a flat film into a kirigami "ZJU" with infrared heating.
Movie S5. Recovery from a flat film into an origami bird with infrared heating.
Fig. S1. Differential scanning calorimeter (DSC) curve for the polymer network.
Fig. S2. Dynamic mechanical analysis (DMA) curve for the polymer network.
Fig. S3. Stress strain curves (five tests) for the polymer network at 70°C (above its melting point), showing that the maximum strain is roughly between 750% and above 1100%.

REFERENCES AND NOTES

1. E. Lee, S. Yang, Bio-inspired responsive polymer pillar arrays. *MRS Commun.* **5**, 97–114 (2015).
2. T. H. Ware, M. E. McConney, J. J. Wie, V. P. Tondiglia, T. J. White, Voxelated liquid crystal elastomers. *Science* **347**, 982–984 (2015).
3. J. Kim, J. A. Hanna, M. Byun, C. D. Santangelo, R. C. Hayward, Designing responsive buckled surfaces by halftone gel lithography. *Science* **335**, 1201–1205 (2012).
4. C. Ma, T. Li, Q. Zhao, X. Yang , J. Wu , Y. Luo , T. Xie, Supramolecular Lego assembly towards three-dimensional multi-responsive hydrogels. *Adv. Mater.* **26**, 5665–5669 (2014).
5. K. M. Lee, T. J. Bunning, T. J. White, Autonomous, hands-free shape memory in glassy, liquid crystalline polymer networks. *Adv. Mater.* **24**, 2839–2843 (2012).
6. R. R. Kohlmeyer, P. R. Buskohl, J. R. Deneault, M. F. Durstock, R. A. Vaia, J. Chen, Shape-reprogrammable polymers: Encoding, erasing, and re-encoding. *Adv. Mater.* **26**, 8114–8119 (2014).
7. H. Koerner, G. Price, N. A. Pearce, M. Alexander, R. A. Vaia, Remotely actuated polymer nanocomposites—Stress-recovery of carbon-nanotube-filled thermoplastic elastomers. *Nat. Mater.* **3**, 115–120 (2004).

Downloaded from http://advances.sciencemag.org/ on January 26, 2016

8. T. Xie, Recent advances in polymer shape memory. *Polymer* **52**, 4985–5000 (2011).
9. M. Behl, M. Y. Razzaq, A. Lendlein, Multifunctional shape-memory polymers. *Adv. Mater.* **22**, 3388–3410 (2010).
10. P. T. Mather, X. Luo, I. A. Rousseau, Shape memory polymer research. *Annu. Rev. Mater. Res.* **39**, 445–471 (2009).
11. A. Lendlein, M. Behl, B. Hiebl, C. Wischke, Shape-memory polymers as a technology platform for biomedical applications. *Expert Rev. Med. Devices* **7**, 357–379 (2010).
12. R. Wang, X. Xiao, T. Xie, Viscoelastic behavior and force nature of thermo-reversible epoxy dry adhesives. *Macromol. Rapid Commun.* **31**, 295–299 (2010).
13. H. Xu, C. Yu, S. Wang, V. Malyarchuk, T. Xie, J. A. Rogers, Deformable, programmable, and shape-memorizing micro-optics. *Adv. Funct. Mater.* **23**, 3299–3306 (2013).
14. I. Bellin, S. Kelch, R. Langer, A. Lendlein, Polymeric triple-shape materials. *Proc. Natl. Acad. Sci. U.S.A.* **103**, 18043–18047 (2006).
15. T. Xie, Tunable polymer multi-shape memory effect. *Nature* **464**, 267–270 (2010).
16. Z. He, N. Satarkar, T. Xie, Y.-T. Cheng, J. Z. Hilt, Remote controlled multishape polymer nanocomposites with selective radiofrequency actuations. *Adv. Mater.* **23**, 3192–3196 (2011).
17. M. Behl, K. Kratz, J. Zotzmann, U. Nöchel, A. Lendlein, Reversible bidirectional shape-memory polymers. *Adv. Mater.* **25**, 4466–4469 (2013).
18. T. F. Scott, A. D. Schneider, W. D. Cook, C. N. Bowman, Photoinduced plasticity in cross-linked polymers. *Science* **308**, 1615–1617 (2005).
19. C. J. Kloxin, T. F. Scott, H. Y. Park, C. N. Bowman, Mechanophotopatterning on a photoresponsive elastomer. *Adv. Mater.* **23**, 1977–1981 (2011).
20. P. Zheng, T. J. McCarthy, A surprise from 1954: Siloxane equilibration is a simple, robust, and obvious polymer self-healing mechanism. *J. Am. Chem. Soc.* **134**, 2024–2027 (2012).
21. D. Montarnal, M. Capelot, F. Tournilhac, L. Leibler, Silica-like malleable materials from permanent organic networks. *Science* **334**, 965–968 (2011).
22. Y.-X. Lu, F. Tournilhac, L. Leibler, Z. Guan, Making insoluble polymer networks malleable via olefin metathesis. *J. Am. Chem. Soc.* **134**, 8424–8427 (2012).
23. M. Capelot, M. M. Unterlass, F. Tournilhac, L. Leibler, Catalytic control of the vitrimer glass transition. *ACS Macro Lett.* **1**, 789–792 (2012).
24. P. Taynton, K. Yu, R. K. Shoemaker, Y. Jin, H. J. Qi, W. Zhang, Heat- or water-driven malleability in a highly recyclable covalent network polymer. *Adv. Mater.* **26**, 3938–3942 (2014).
25. J. P. Brutman, P. A. Delgado, M. A. Hillmyer, Polylactide vitrimers. *ACS Macro Lett.* **3**, 607–610 (2014).
26. Z. Pei, Y. Yang, Q. Chen, E. M. Terentjev, Y. Wei, Y. Ji, Mouldable liquid-crystalline elastomer actuators with exchangeable covalent bonds. *Nat. Mater.* **13**, 36–41 (2014).
27. B. T. Michal, C. A. Jaye, E. J. Spencer, S. J. Rowan, Inherently photohealable and thermal shape-memory polydisulfide networks. *ACS Macro Lett.* **2**, 694–699 (2013).
28. E. D. Rodriguez, X. Luo, P. T. Mather, Linear/network poly(ε-caprolactone) blends exhibiting shape memory assisted self-healing (SMASH). *ACS Appl. Mater. Interfaces* **3**, 152–161 (2011).
29. A. Lendlein, R. Langer, Biodegradable, elastic shape-memory polymers for potential biomedical applications. *Science* **296**, 1673–1676 (2002).
30. J.-H. Na, A. A. Evans, J. Bae, M. C. Chiappelli, C. D. Santangelo, R. J. Lang, T. C. Hull, R. C. Hayward, Programming reversibly self-folding origami with micropatterned photocrosslinkable polymer trilayers. *Adv. Mater.* **27**, 79–85 (2015).
31. S. M. Felton, M. T. Tolley, B. Shin, C. D. Onal, E. D. Demaine, D. Rus, R. J. Wood, Self-folding with shape memory composites. *Soft Matter* **9**, 7688–7694 (2013).
32. Y. Luo, Y. Guo , X. Gao , B.-G. Li , T. Xie, A general approach towards thermoplastic multishape-memory polymers via sequence structure design. *Adv. Mater.* **25**, 743–748 (2013).
33. T. Xie, K. A. Page, S. A. Eastman, Strain-based temperature memory effect for Nafion and its molecular origins. *Adv. Funct. Mater.* **21**, 2057–2066 (2011).
34. H. Kweon, M. K. Yoo, I. K. Park, T. H. Kim, H. C. Lee, H. S. Lee, J. S. Oh, T. Akaike, C. S. Cho, A novel degradable polycaprolactone networks for tissue engineering. *Biomaterials* **24**, 801–808 (2003).

Acknowledgments: We acknowledge H. Bai and J. Wu for their kindly help with the discussions. **Funding:** This work was supported by the following programs: National Key Basic Research Program of China (no. 2015CB351903), National Natural Science Foundation of China (nos. 21474084 and 21470490), the Chinese central government's Recruitment Program of Global Experts, and 985 program for the startup funding. **Author contributions:** T.X. conceived the concept and wrote the paper. Q.Z. designed the experiments. Q.Z. and W.Z. conducted the experiments. T.X. and Y.L. directed the project. All authors analyzed and interpreted data. **Competing interests:** The authors declare that they have no competing interests. **Data and materials availability:** All data needed to evaluate the conclusions in the paper are present in the paper and/or the Supplementary Materials. Additional data related to this paper may be requested from the authors.

Submitted 17 September 2015
Accepted 13 November 2015
Published 8 January 2016
10.1126/sciadv.1501297

Citation: Q. Zhao, W. Zou, Y. Luo, T. Xie, Shape memory polymer network with thermally distinct elasticity and plasticity. *Sci. Adv.* **2**, e1501297 (2016).

Downloaded from http://advances.sciencemag.org/ on January 26, 2016

ScienceAdvances
AAAS

Shape memory polymer network with thermally distinct elasticity and plasticity

Qian Zhao, Weike Zou, Yingwu Luo and Tao Xie (January 8, 2016)

Sci Adv 2016, 2:.
doi: 10.1126/sciadv.1501297

This article is publisher under a Creative Commons license. The specific license under which this article is published is noted on the first page.

For articles published under CC BY licenses, you may freely distribute, adapt, or reuse the article, including for commercial purposes, provided you give proper attribution.

For articles published under CC BY-NC licenses, you may distribute, adapt, or reuse the article for non-commerical purposes. Commercial use requires prior permission from the American Association for the Advancement of Science (AAAS). You may request permission by clicking here.

The following resources related to this article are available online at http://advances.sciencemag.org. (This information is current as of January 26, 2016):

Updated information and services, including high-resolution figures, can be found in the online version of this article at:
http://advances.sciencemag.org/content/2/1/e1501297.full

Supporting Online Material can be found at:
http://advances.sciencemag.org/content/suppl/2016/01/05/2.1.e1501297.DC1

This article **cites 34 articles,**6 of which you can be accessed free:
http://advances.sciencemag.org/content/2/1/e1501297#BIBL

Downloaded from http://advances.sciencemag.org/ on January 26, 2016

Science Advances (ISSN 2375-2548) publishes new articles weekly. The journal is published by the American Association for the Advancement of Science (AAAS), 1200 New York Avenue NW, Washington, DC 20005. Copyright is held by the Authors unless stated otherwise. AAAS is the exclusive licensee. The title Science Advances is a registered trademark of AAAS